

COST ACTION ES1005 TOSCA
RECENT VARIABILITY OF THE SOLAR SPECTRAL IRRADIANCE
AND ITS IMPACT ON CLIMATE MODELLING



Spectral Irradiance reconstructions based on intensity images

Ilaria Ermolli

INAF Osservatorio Astronomico di Roma

Freie Universität, Berlin, 14-16 May 2012

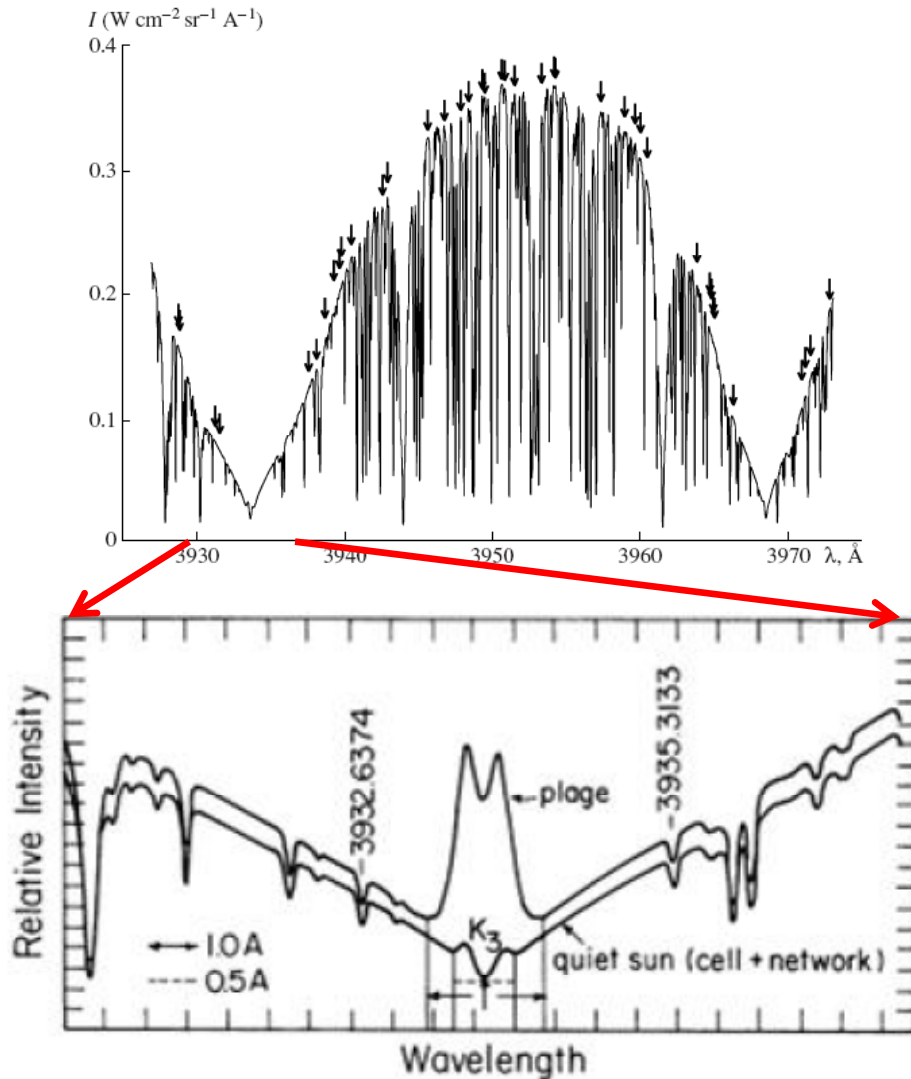


This talk

- Ca II K as a magnetic field proxy
- Results in the literature
 - Regression methods based on full-disk observations (SFO)
 - Models based on RT, semi-empirical atm models and full-disk obs (SRPM)
- Results of a model based on RT, semi-empirical atm models and full-disk obs
 - TSI , SSI
 - disk-integrated intensity and feature contrast



Ca II K as a magnetic field proxy



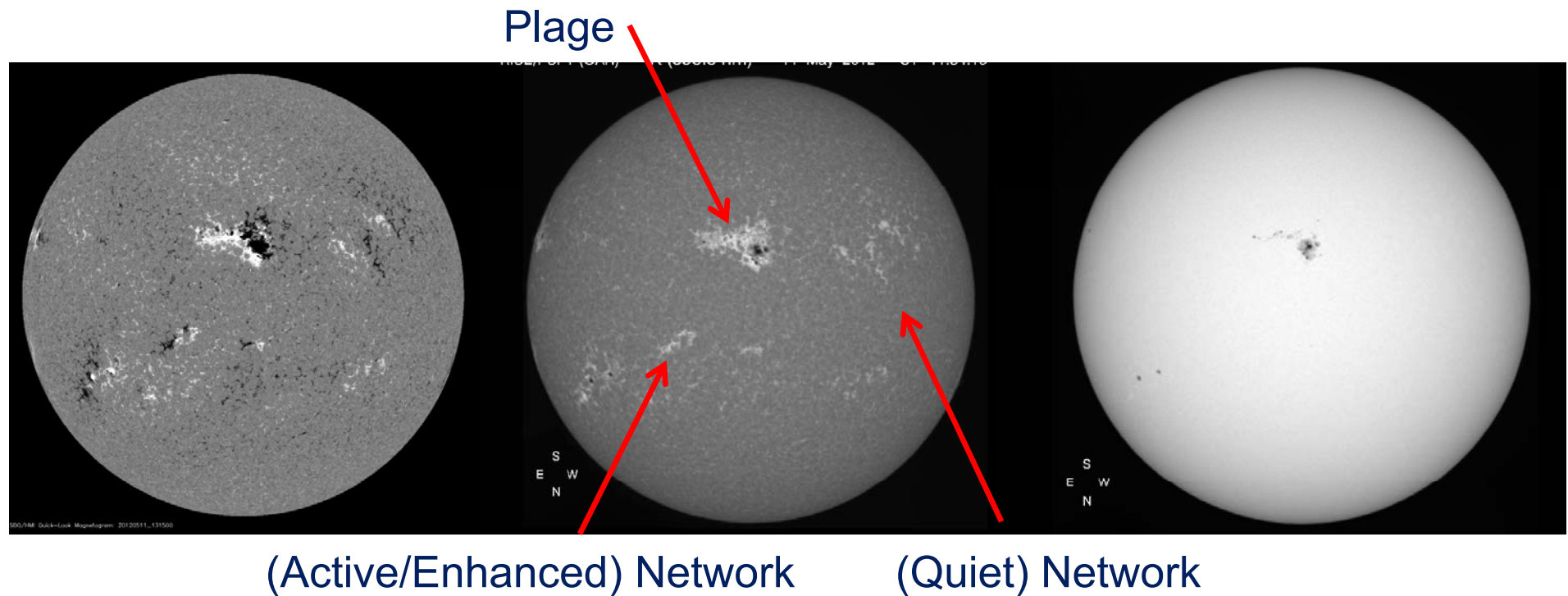
Ca II H and Ca II K lines become brighter with non-spot magnetic flux.

$$I_{\text{core}}/I_{\text{wing}} \approx \langle B \rangle^{0.6}$$



Ca II K as a magnetic field proxy

Non-spot magnetic regions appear bright in Ca II H and Ca II K:





Results in the literature

- Regression methods based on full-disk observations

SFO method

- Models based on RT computations, semi-empirical atm models and full-disk PSPT observations

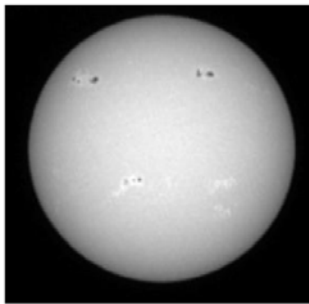
SRPM based on SRPM and PSPT



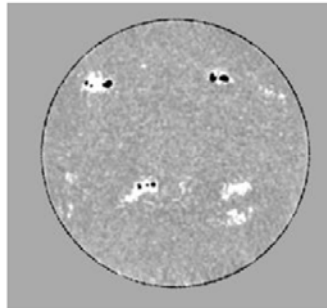
SFO method

Image Analysis

Observed image



Contrast image



I_i : intensity of pixel i

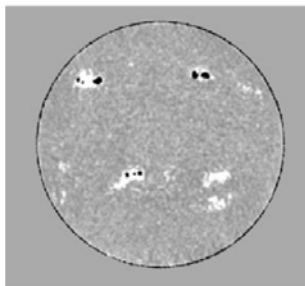
$I_{\text{Quiet-Sun}}$: function of μ

C_i : contrast of pixel i

$$C_i = \frac{I_i}{I_{\text{Quiet-Sun}}} - 1$$

Photometric Sum, Σ_λ

Contrast image



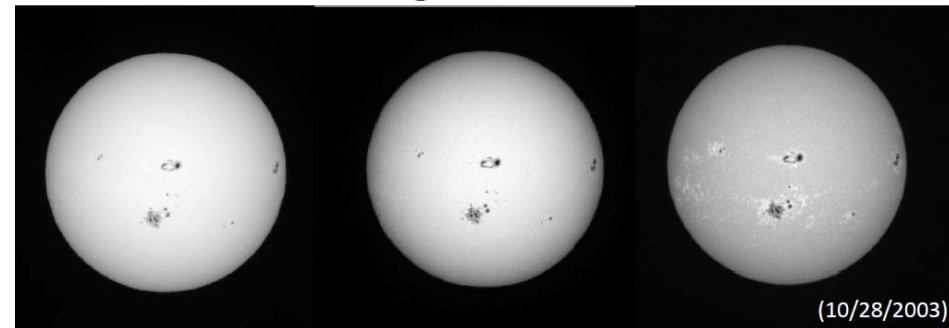
$$\Sigma_\lambda = \sum_{\text{all pixels } i} C_{i,\lambda} \phi_{i,\lambda}$$

$\phi_{i,\lambda}$: Quiet-Sun limb-darkening, normalized to unit integral over the disk

Σ_λ : relative contribution of solar features to the disk-integrated intensity [ppm of quiet-Sun]

- Includes low contrast features (above noise)

San Fernando Observatory Daily images for 22 years



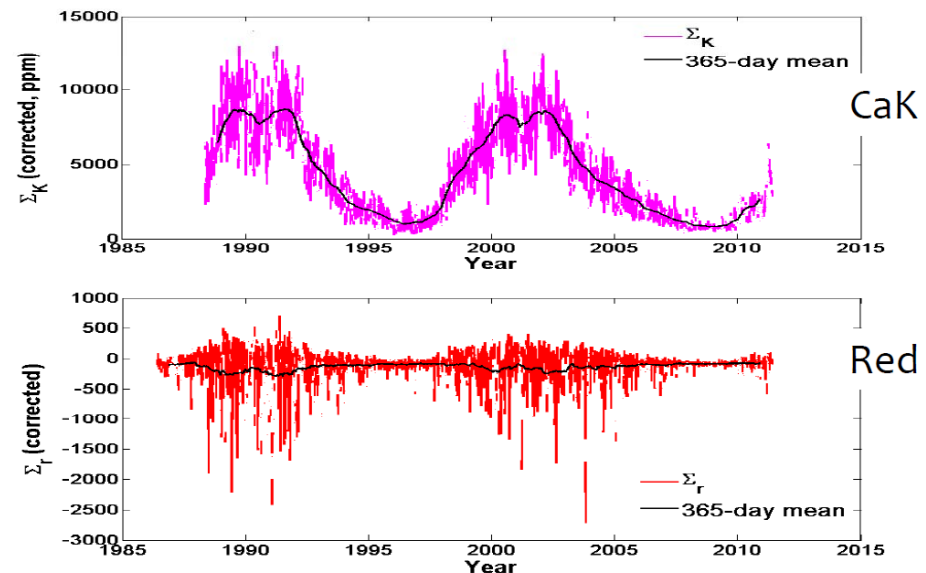
(10/28/2003)

Red
672.3 nm
Continuum
photosphere

Blue
472.3 nm
Continuum
photosphere

Ca II K
393.4 nm
Spectral Line
low chromosphere

Σ_r and Σ_K (corrected for bias)

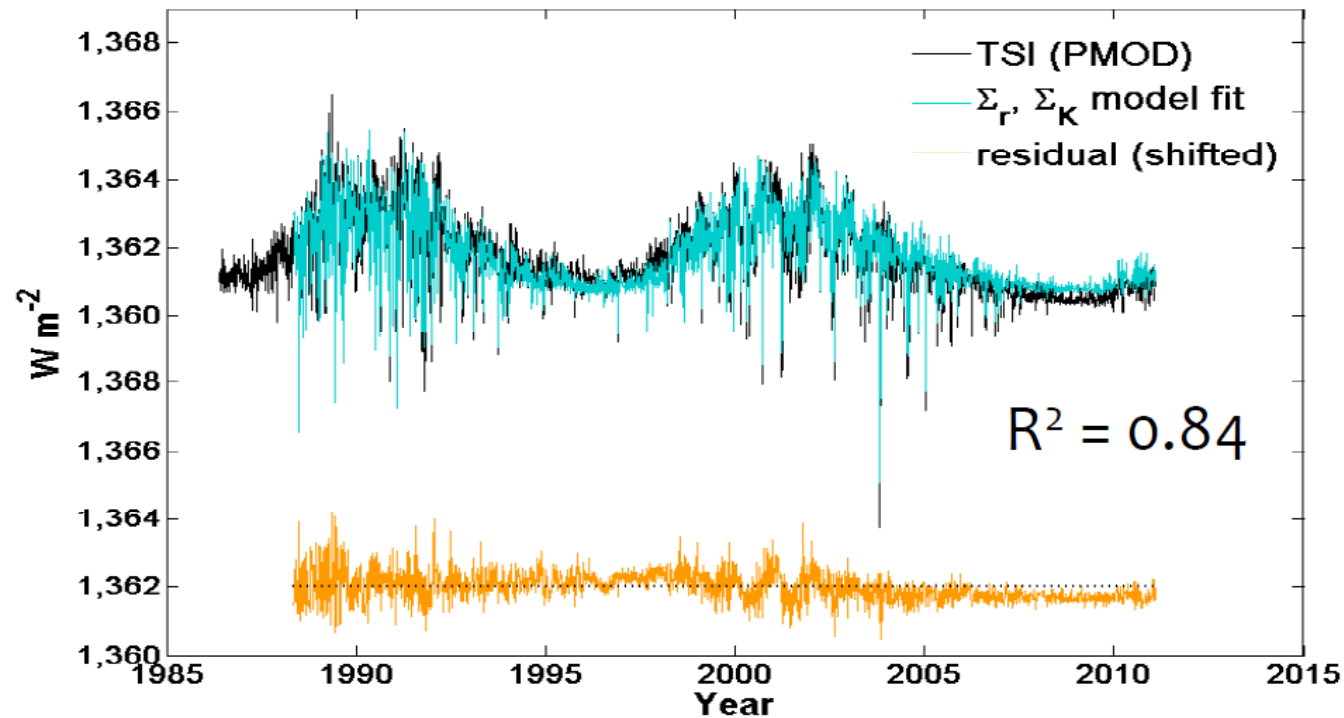


Courtesy: D. Preminger



SFO method

$$\text{Model: } \text{TSI}(t) = \text{TSI}_0 [1 + a_1 \cdot \Sigma_r(t) + a_2 \cdot \Sigma_K(t)]$$



Model assumes that Quiet Sun is constant
 ΔTSI is due to entirely to solar features

10



SFO method

Preminger et al. 2011, ApJ, 739, L45

“The bolometric and spectral line brightness are strongly enhanced by solar activity, on the order of 0.1% at solar maximum, while continuum brightness is slightly diminished, on the order of – 0.02%.”

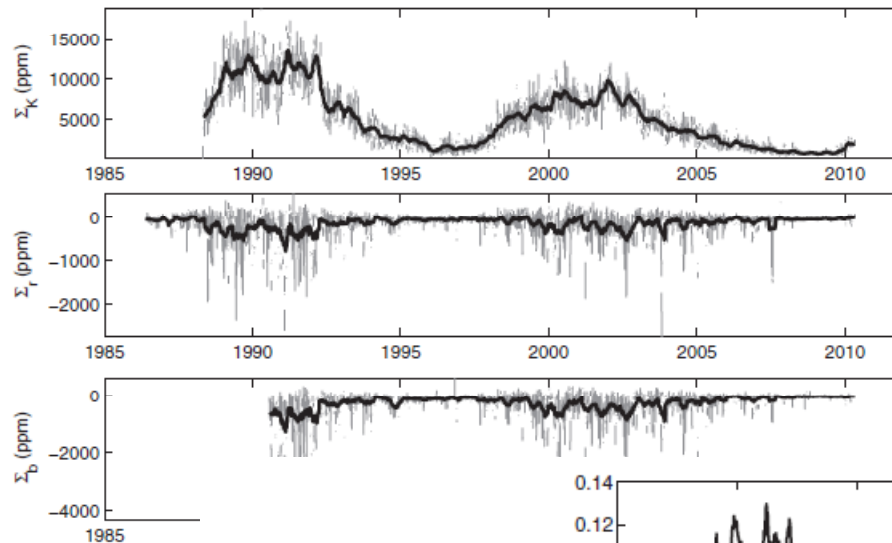


Figure 2. Top: the Ca II K-line photometric sum, photometric sum, Σ_b , from blue continuum image of solar features. The bold curves are the 81 day

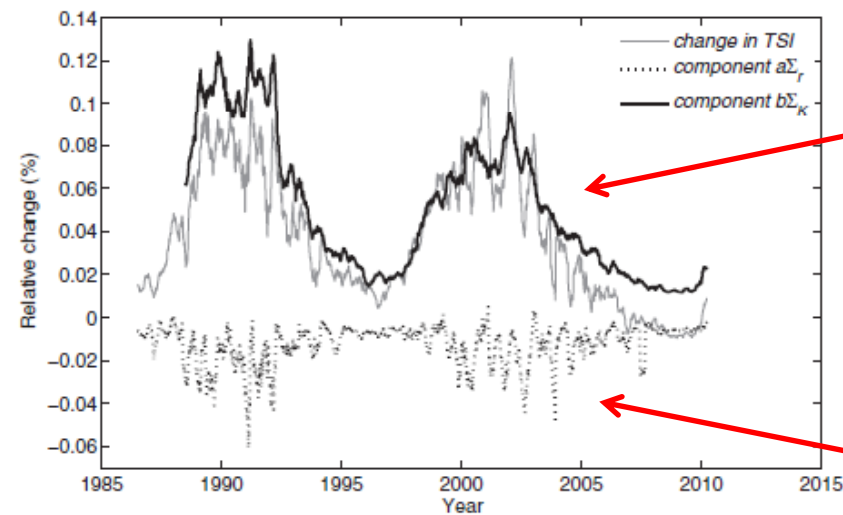


Figure 5. 81 day running mean of the relative change in TSI and the two primary contributing components. We infer that $a\Sigma_r$ represents the change in continuum irradiance and $b\Sigma_K$ represents the change in spectral lines. Here, the components have been corrected for the effects of quiet-Sun bias.



SRPM model

SRPM Solar Radiation Physical Modeling

Fontenla et al. 1999 → Fontenla et al. 2009, Fontenla et al. 2011

Input:

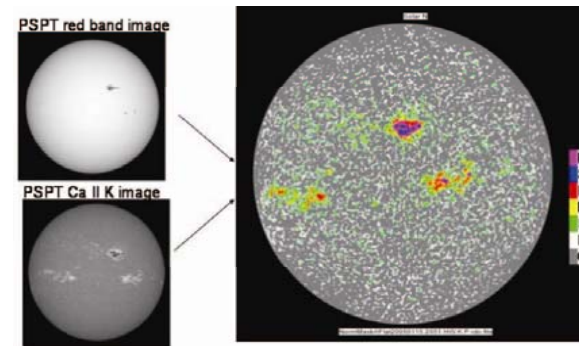
1) magnetic field distribution from Ca II K observations (PSPT images);

2) spectra of photospheric components (semi-empirical model atmospheres)

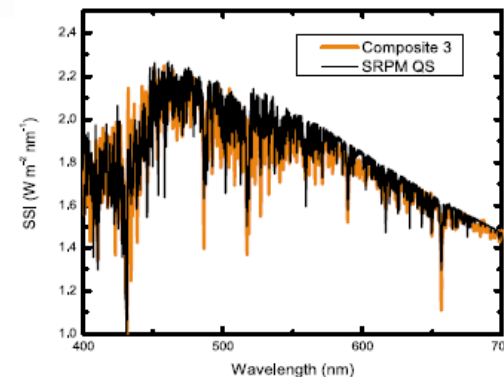
Output: solar total and spectral irradiance vs. Time, spectra at given times

Main features:

- SRPM (NLTE computations) + Fontenla 2011
- Free parameters: 0
- n (>7)- Component model



1 (2)
arcsec/pix
0.1% photom
accuracy



Emergent
intensity
const vs
time



SRPM model

SRPM HR SSI computations

Fontenla et al. 2011, JGR, 116, D2010

Table 1. Solar Features Designation and Corresponding Model Indices

Feature	Description	Photosphere-Chromosphere Model Index	Corona Model Index
A	Dark quiet-Sun inter-network	1000	1010
B	Quiet-Sun inter-network	1001	1011
D	Quiet-Sun network lane	1002	1012
F	Enhanced network	1003	1013
H	Plage (that is not facula)	1004	1014
P	Facula (i.e., very bright plage)	1005	1015
S	Sunspot umbra	1006	1016
R	Sunspot penumbra	1007	1017
Q	Hot facula	1008	1018

Improvements were done in the models in order to better match the **SORCE/SIM** data shown by Harder et al. 2009

Change of the photospheric/low-chromospheric temperature derivative with respect to pressure of the various feature models.

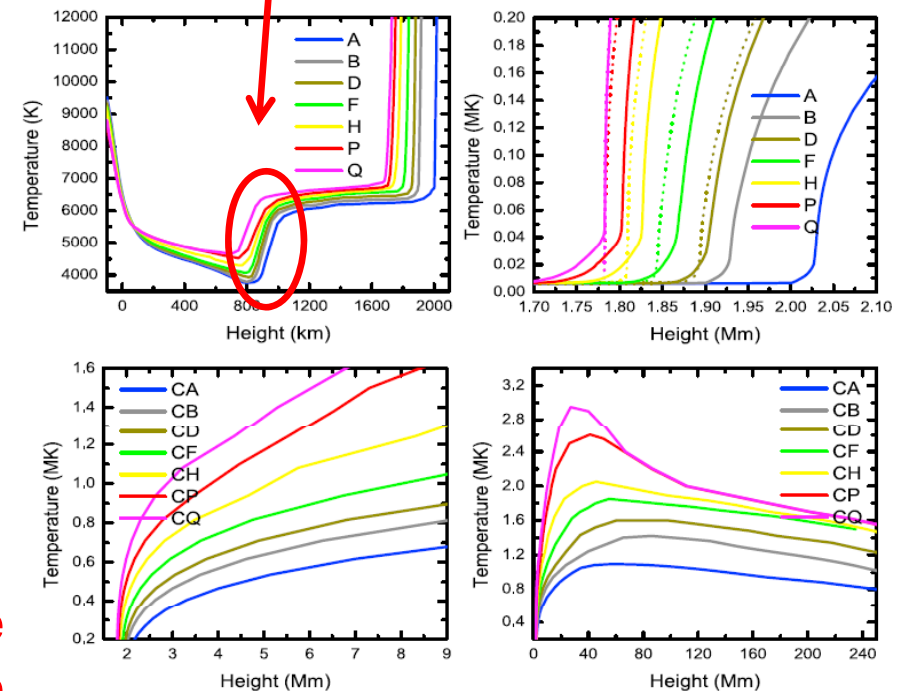


Figure 1. Temperature vs. height for the solar atmospheric features. Dotted lines correspond to models of footpoints of coronal loops (see Section 5.5), and solid lines correspond to the final models adopted. (top left) The entire photosphere and chromosphere for the models representing various solar features as indicated in Table 1. (top right) The detail of the lower transition-region for the models representing various solar features as indicated in Table 1. (bottom left) The detail of the upper transition-region for the models representing various solar features as indicated in Table 1. (bottom right) The coronal portions of the models as indicated in Table 1.



SRPM model

SRPM HR SSI computations

Fontenla et al. 2011, JGR, 116, D2010

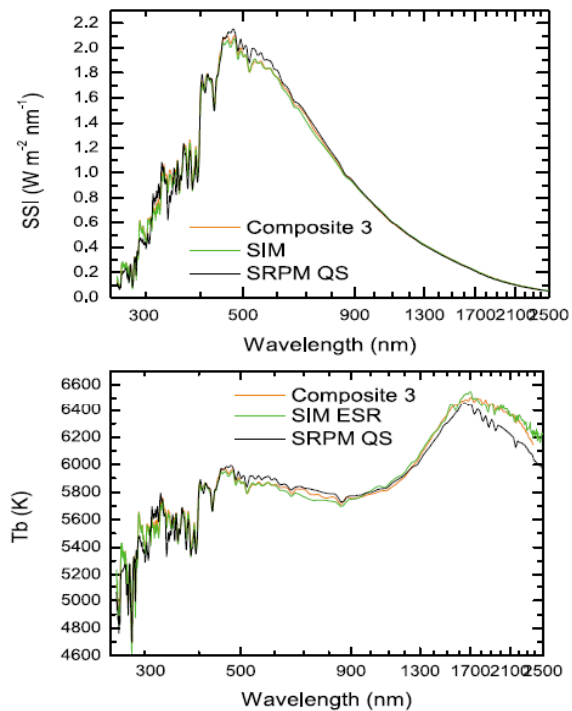


Figure 16. Comparison of the SRPM QS and the *Thuillier et al. [2003]* Composite 3 spectra with the SORCE/SIM ESR detector observation on 2004/4/21. Convolution of the SRPM and Composite 3 was made with the variable SIM instrument profile. (top) In standard SSI units and (bottom) in brightness temperature that highlights the differences.

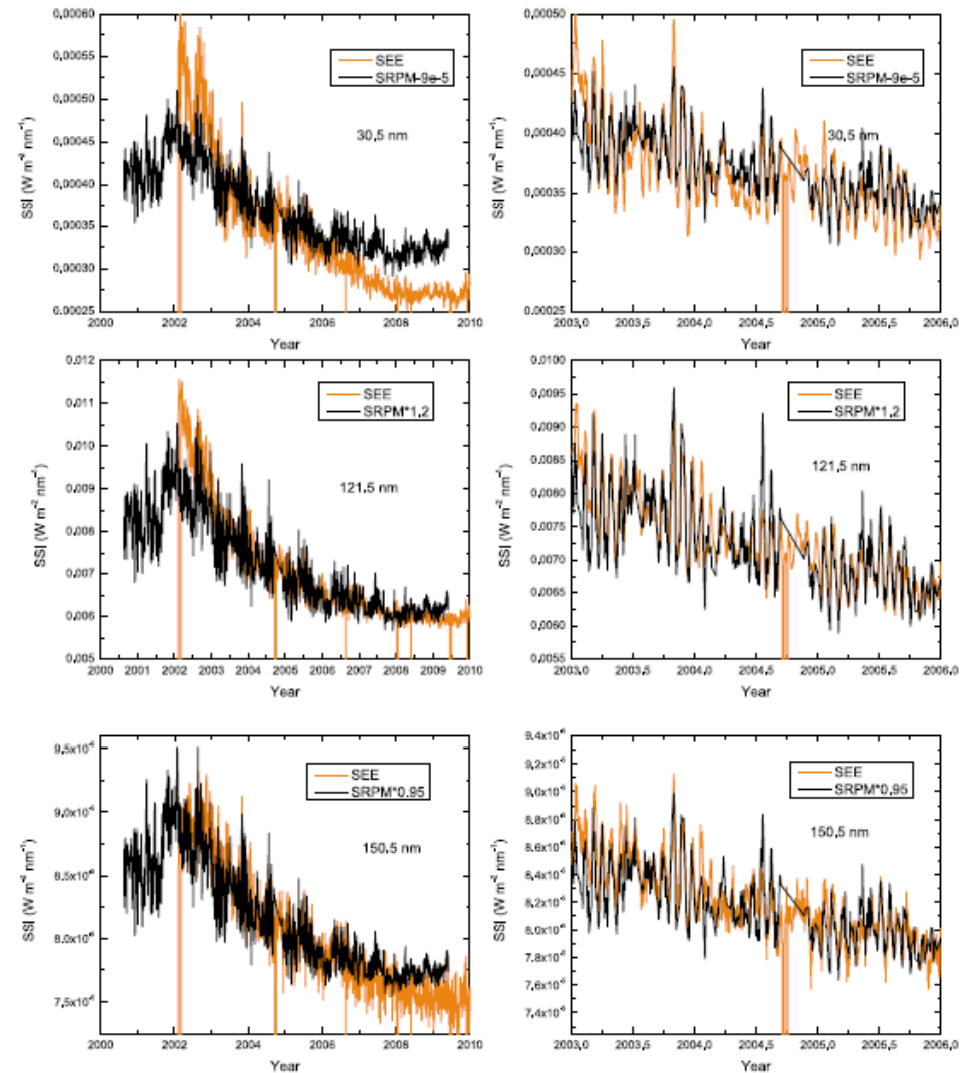


Figure 20. Samples of the Solar Cycle 23 and the rotational modulation of the EUV and FUV comparison between TIMED/SEE and the SRPM calculations. These wavelengths are dominated by chromospheric and low transition-region emissions.



SRPM model

SRPM HR SSI computations

Fontenla et al. 2011, JGR, 116,
D2010

“There is another component that affects the bolometric flux but which is not yet considered by SRPM, this factor is not related to rotational modulation. The same issue also applies to the SSI.”

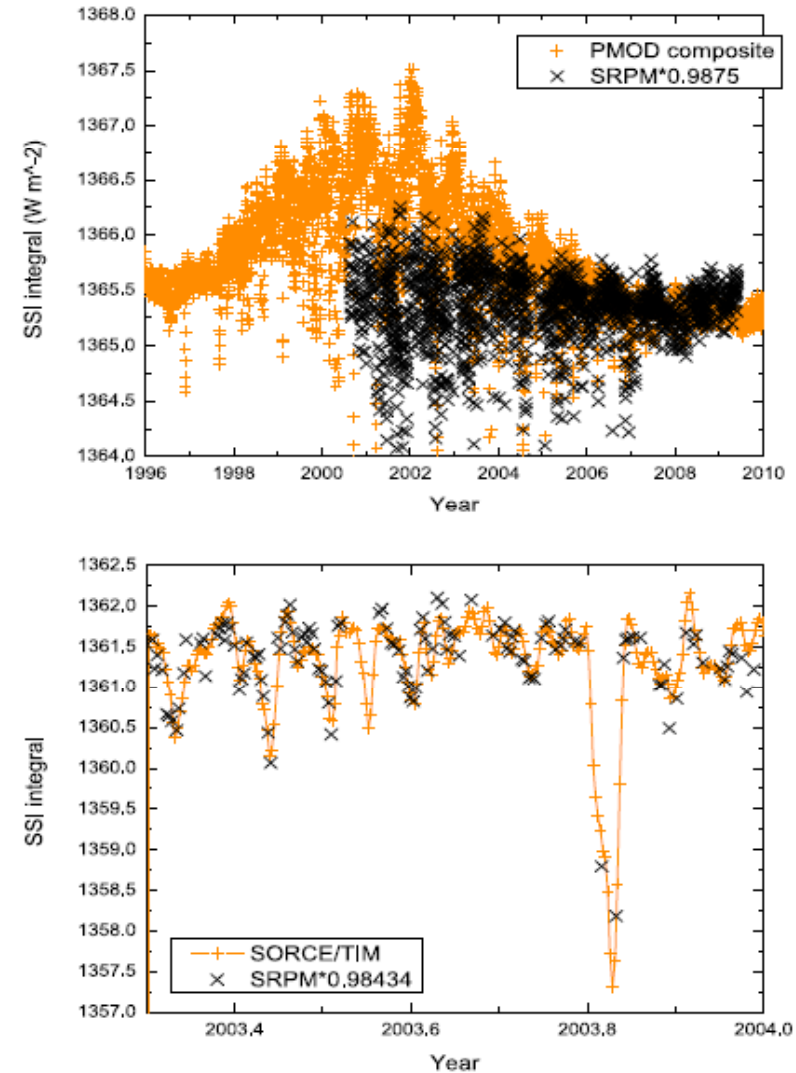


Figure 23. Comparison of the bolometric flux computed by SRPM with published TSI composite observations. (top) The full Solar Cycle 23 from the PMOD composite, and (bottom) an enlargement of the period 2003–2004 from SORCE/TIM. The short-lived large decreases of the TSI are due to large sunspot groups and particularly the drop around 2003 October 28 is due to the very large sunspot complex that produced the “Halloween” flare mentioned in Section 6.



Similar model

SRPM semi-empirical model atmospheres, RH (NLTE) RT code, PSPT observations

Input:

1) magnetic field distribution from Ca II K observations (PSPT images);

2) spectra of photospheric components (semi-empirical model atmospheres)

Output: solar total and spectral irradiance vs. time, contrast of features vs. time

Main features:

- RH (NLTE computations) + Fontenla 2009
- Free parameters: 0
- 7- Component model

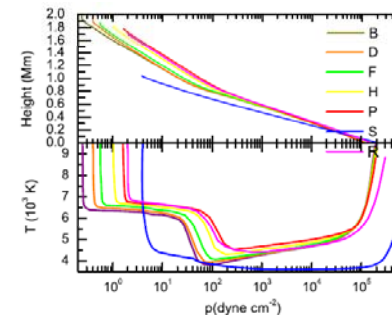
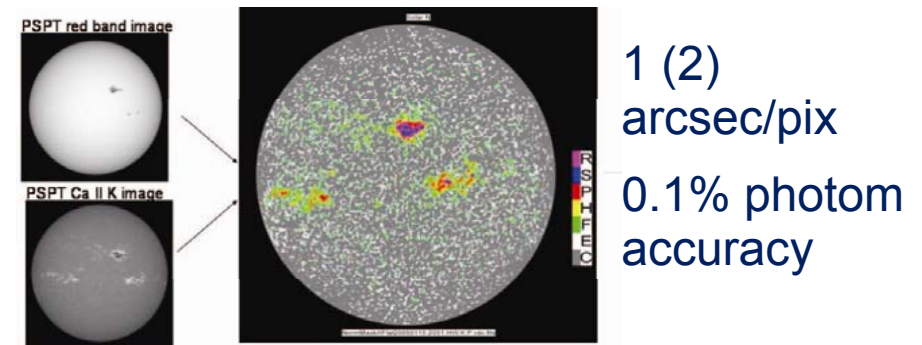


Figure 2. Temperature and height of the layers as functions of pressure for the models in Table 1. The increased slope of the height vs. pressure, at pressures below that of the temperature minimum, corresponds to a larger height-scale due to increased temperature and non-thermal acceleration in the upper chromospheres.

Emergent intensity const vs time



SRPM model

SRPM semi-empirical model atmospheres

Fontenla et al. 2009, ApJ, 707, 482

Designation of Features

Feature designation	Model index	Feature Description	Pressure at 2×10^5 K (dyne cm ⁻²)
B	1001	Quiet-Sun inter-network	0.235
D	1002	Quiet-Sun network lane	0.340
F	1003	Enhanced network	0.552
H	1004	Plage (that is not facula)	1.00
P	1005	Facula (i.e., very bright plage)	1.62
S	1006	Sunspot umbra	3.86
R	1007	Sunspot penumbra	2.10

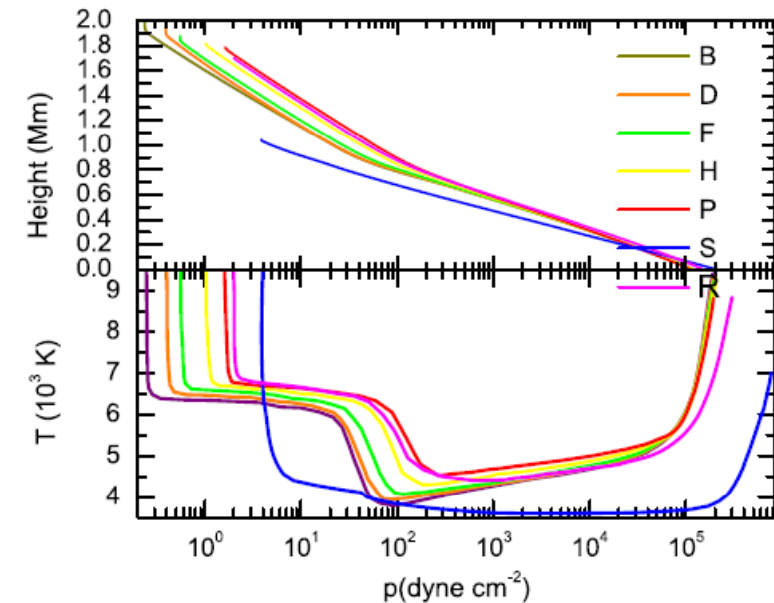
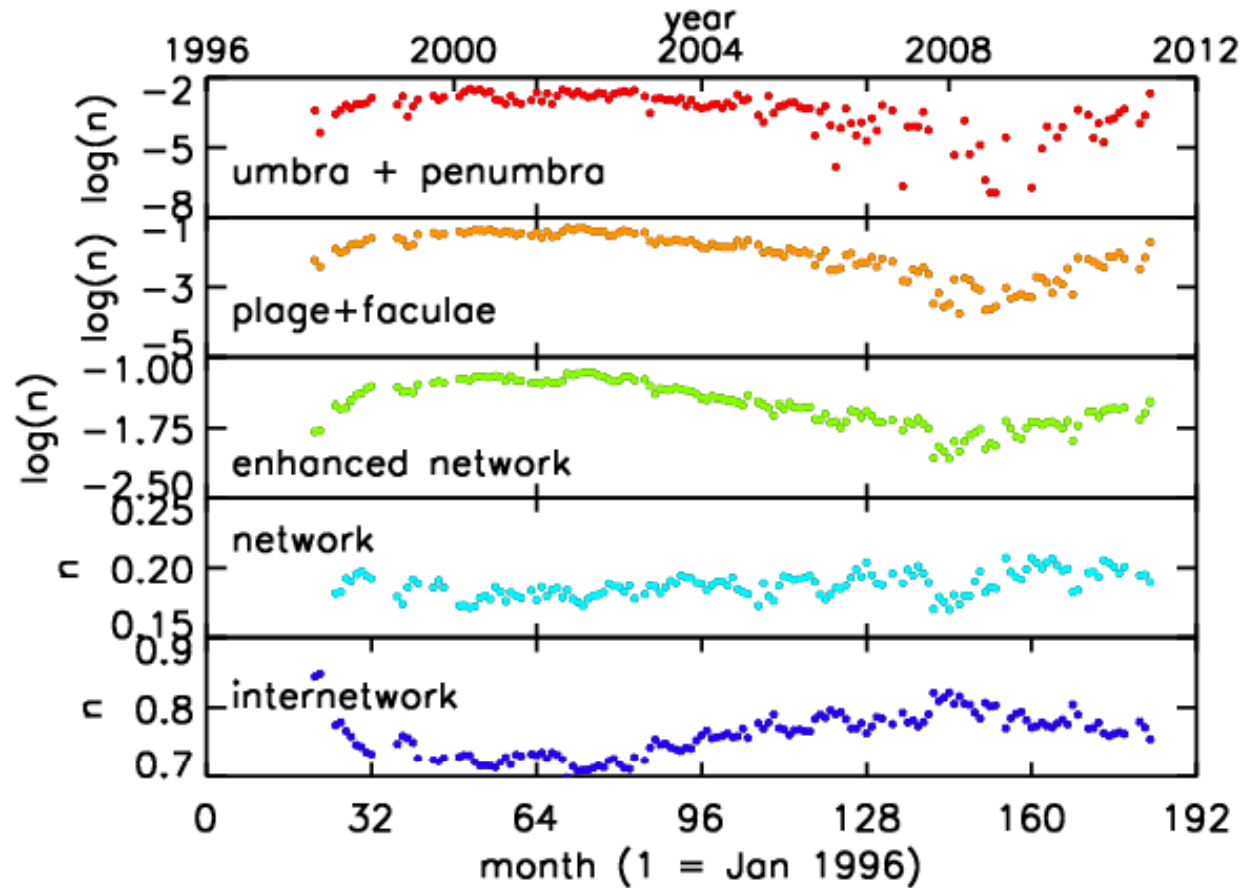


Figure 2. Temperature and height of the layers as functions of pressure for the models in Table 1. The increased slope of the height vs. pressure, at pressures below that of the temperature minimum, corresponds to a larger height-scale due to increased temperature and non-thermal acceleration in the upper chromospheres.



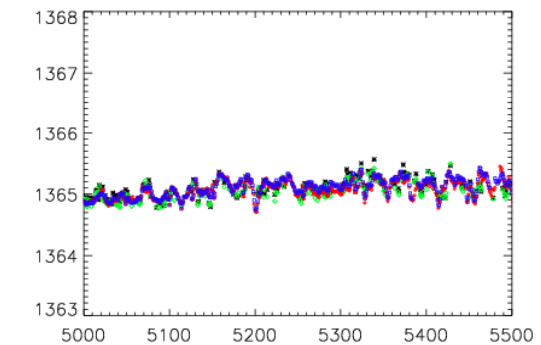
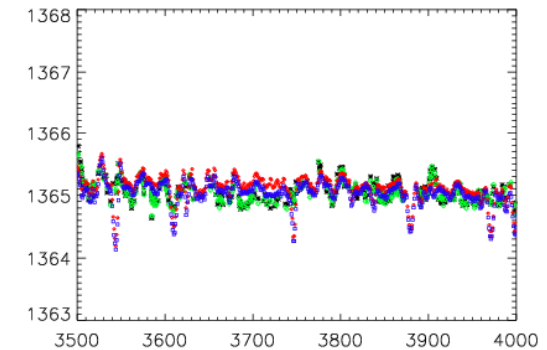
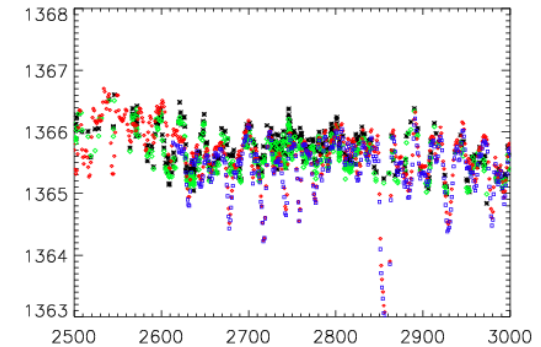
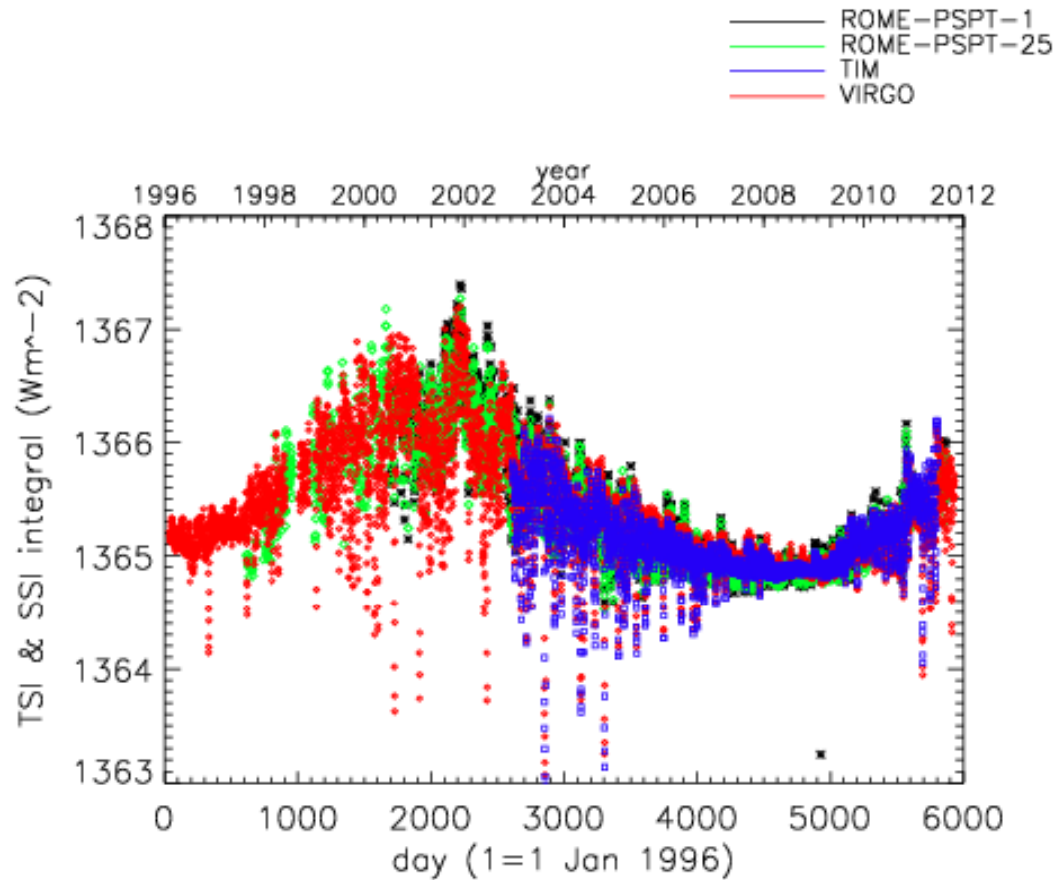
Rome-PSPT measurements



Fractional solar disk area covered by magnetic and non-magnetic features.



Rome model

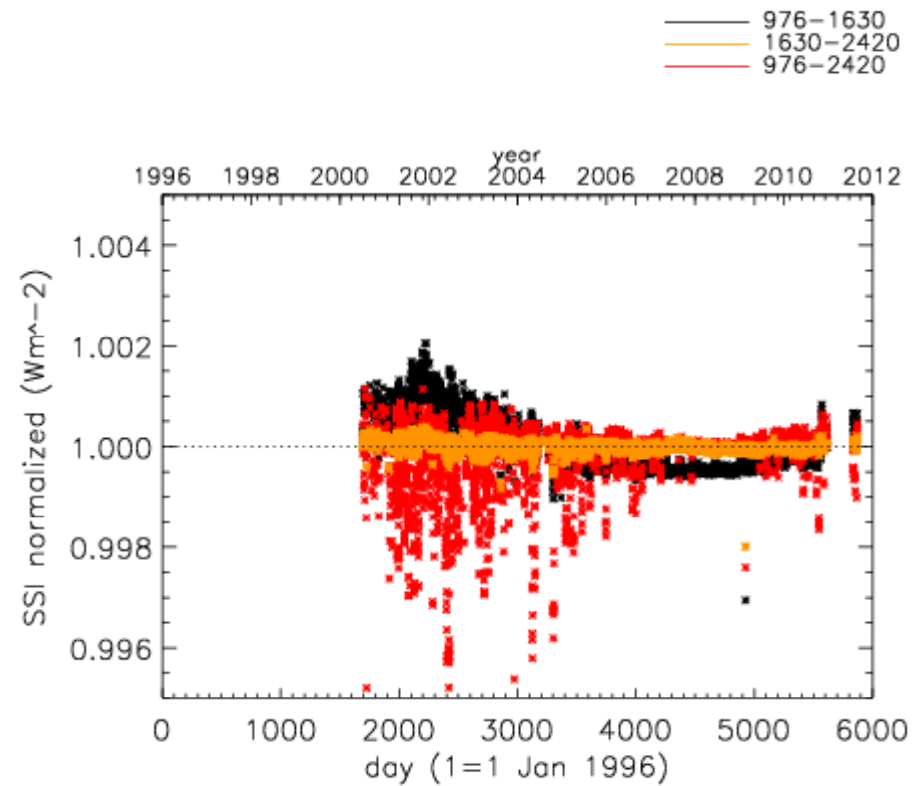
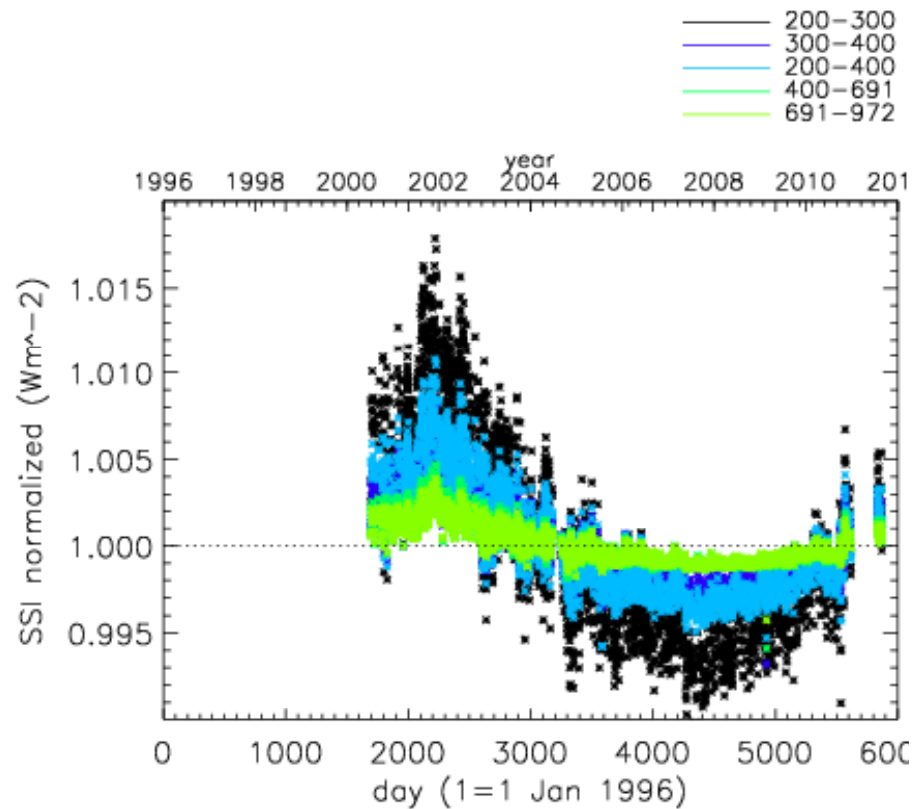


Comparison between daily values of TSI measured by VIRGO and TIM and those obtained with the model.



Rome model

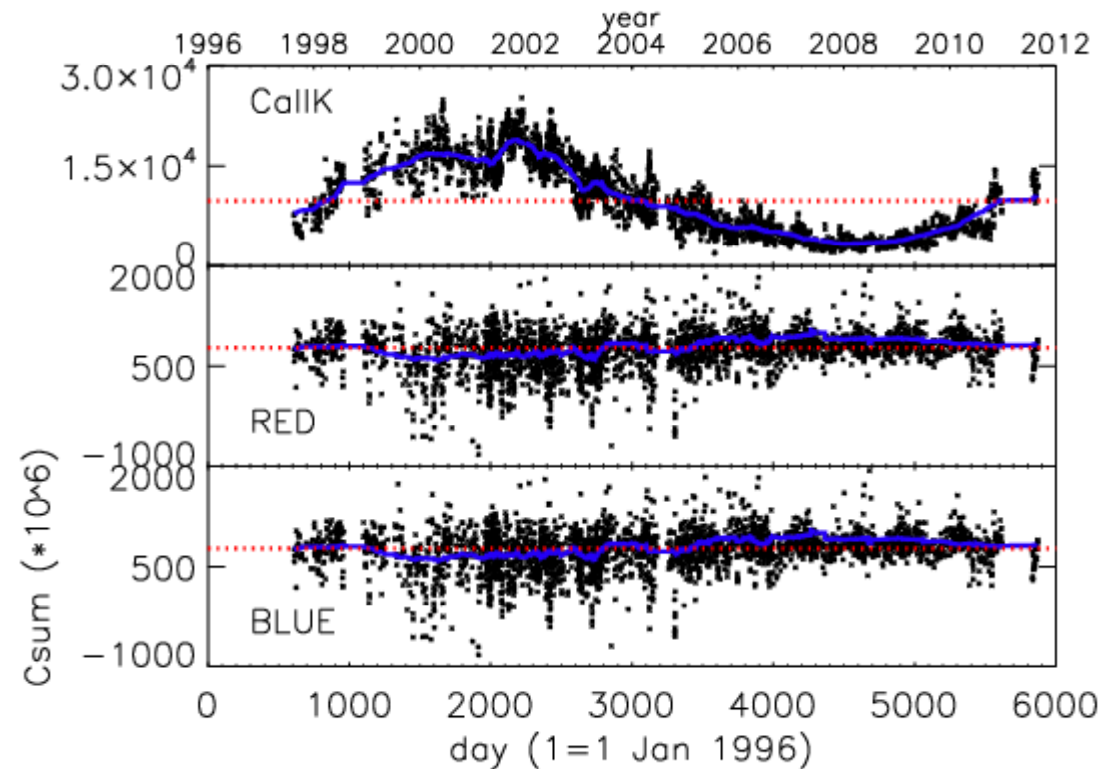
SSI Aug 2000 - Jan 2012



Relative variation of SSI over wavelength ranges as a function of time 2000-2012.



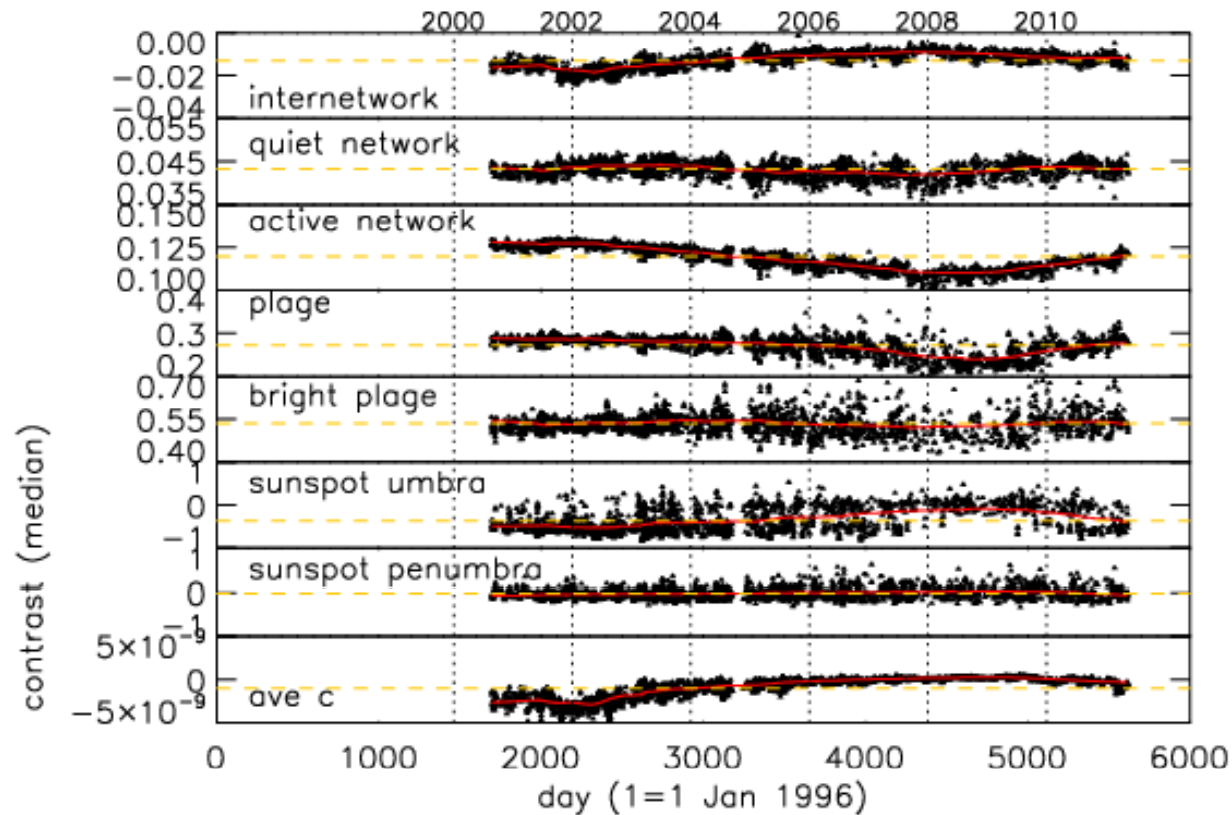
Rome-PSPT measurements



Relative change (in parts per million) in the disk-integrated intensity of the Sun due to the presence of solar features.



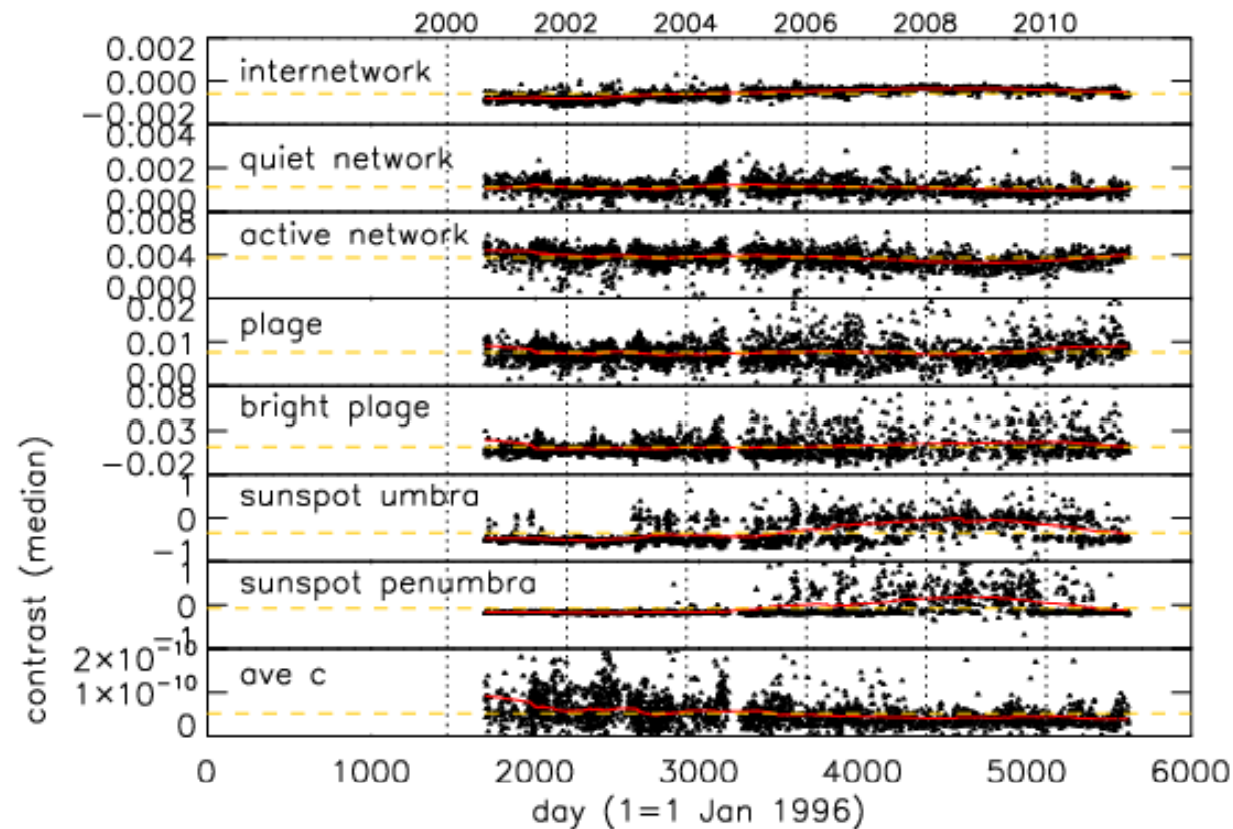
Rome-PSPT measurements



Relative change of the median value of the Ca II K contrast of the various features.



Rome-PSPT measurements



Relative change of the median value of the Red contrast of the various features.



Conclusions

Results derived from the model based on RH computations, SRPM(2009) semi-empirical atm models, and full-disk observations are qualitatively in agreement with those discussed so far.

The (7-component) model is found to be in good agreement with both PMOD/VIRGO and SORCE/TIM measurements on both rotational and cyclic time scales. Trends of SSI integrated over wave ranges oppose SORCE/SIM results in the visible (400-691 nm) and NIR (976-1630 nm, 976-2420 nm)

The bolometric and spectral line brightness are (strongly) enhanced by solar activity, continuum brightness is (slightly/barely) diminished.